Modified shallow water equations for inviscid gravity currents

An-Cheng Ruo and Falin Chen
Institute of Applied Mechanics, National Taiwan University, Taipei, Taiwan 106
(Received 24 December 2005; revised manuscript received 30 October 2006; published 5 February 2007)

To analyze the motion of gravity current, a common approach is to solve the hyperbolic shallow water equations (SWE) together with the boundary conditions at both the current source at far upstream (i.e., the constrained condition) and the current front at downstream margin (i.e., the front condition). The use of the front condition is aimed to take the resistance from the ambient fluid into account, because the ambient resistance is absent in the SWE. In the present study, we rederive the SWE by taking the ambient resistance into account and end up with the so-called modified shallow water equation (MSWE). In the MSWE the ambient resistance is given by a nonlinear term, so that the use of the front condition becomes unnecessary. These highly nonlinear equations are approximated by the perturbation expansion to the leading order, and the resultant singular perturbation equations are solved analytically by the inner-outer expansion approach. Results show that for constant-flux and constant-volume gravity currents, their outer solutions are exactly the same as the solutions obtained by solving the SWE with the front condition. The inner solutions give both the profile and the velocity of the current head and lead to the recovery of the front condition in a more general form. The combination of inner and outer solutions gives a composite solution for the whole current, which was called by Benjamin [J. Fluid Mech. **31**, 209 (1968)] a "formidably complicated" task. To take the turbulent drag on the current into account, we introduce the semiempirical Chezy drag term into the MSWE and results agreed with experimental data very well. The MSWE can be extended for three-dimensional gravity currents, while the resultant equations become so complicated that analytical solutions might not be available.

DOI: 10.1103/PhysRevE.75.026302 PACS number(s): 47.15.−x, 44.20.+b

I. INTRODUCTION

A gravity current is a gravity-driven flow intruding horizontally into another fluid. The two fluids are generally of different density due to different temperature (and/or concentration) or insoluble particles suspended in the intruding fluid. In many situations, the motion of gravity current is concerned with human safety and environmental concern, such as the accidental release of toxic dense gas due to the rupture of a storage tank, the powder snow avalanche, the river water discharging into the sea (an upside-down gravity current), …. and so on. The study of gravity current therefore is of considerable importance in natural science and wide applications in engineering. A detailed description of a variety of gravity currents is given in the monograph of Simpson [1].

Some typical gravity currents can be reconstructed in laboratories by using a rectangular box filled with two fluids of different densities separated by a removable lock [2]. As the lock is removed, two fluids intrude each other and the gravity current is generated. A remarkable feature observed is the mixing and entrainment at the current front due to the strong shear stress at the interface between two fluids. The shear stress leads to the so-called Kelvin-Helmholtz instability at the interface, creating a complicated three-dimensional flow called "lobes and clefts" at the current front. Besides, the time-dependent characteristics associated with the initial-state evolution also enhance the complication of the problem. All these characteristics lead to the conclusion that a complete solution for the motion of gravity current, either in theoretical or in numerical form, has long been considered as a formidable task [3].

Even though the gravity current motion appears to be difficult to handle, many previous studies have employed a simplified mathematical model and have successfully revealed key characteristics of the current motion. For example, in the study of atmospheric gravity currents, such as sea-breeze fronts or thunderstorm outflows, the main interest is the prediction of the spreading speed. Observations from early experiments pointed out the current front always approaches a constant speed, which inspired theoretical researchers to assume a steady-state gravity current [3,4]. This steady-state approach proposed by Benjamin [3] has since played a decisive role in theoretical approaches and has come up with a formula that relates the speed of the current front u_f with the height of the current head h_f, given by

$$u_f = \beta\sqrt{g_r h_f}, \tag{1.1}$$

in which $g_r=[(\rho-\rho_a)/\rho]g$ is the reduced gravity, g the gravitational acceleration, ρ the density of the current fluid, and ρ_a the density of the ambient fluid. Note that h_f is not the height at the forefront point x_f (where the height of the current is zero) but is the height just behind the current head x_m (see Fig. 1). The parameter β varies with different situations and is determined by either theoretical or experimental ap-

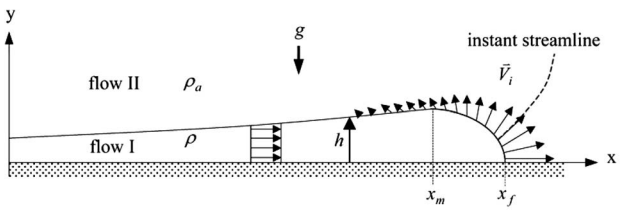

FIG. 1. A schematic description of the gravity current considered.

proaches. Groebelbauer *et al.* [2] neglected viscous effect and used the conservation of mass and momentum to determine its value to be $\sqrt{2/\gamma}$ (where $\gamma \equiv \rho_a/\rho$) for an inviscid gravity current flowing beneath an infinite ambient fluid.

Although the steady-state analysis provides a preliminary solution of the advancing speed of the current front, the evolution at the initial stage is still the most crucial part to understand the thorough behavior of gravity current during its spreading. This is particularly important to oceanographic engineering, such as the spreading of spilled oil and the intrusion of fresh water into the salt water in the vicinity of estuaries. To attack such a transient situation, many theoretical studies [5–13] applied the shallow-water approximation under which the vertical velocity of the current is assumed to be much less than the horizontal velocity at a sufficiently long time after release. As a result, the shallow-water equations (SWE) were derived after assumptions such as the flow is planar or axisymmetric, the two fluids are inviscid, there is no surface tension or mixing at the interface, and so on, were made. The planar SWE can be written as

$$\frac{\partial h}{\partial t} + \frac{\partial (uh)}{\partial x} = 0, \tag{1.2}$$

$$\frac{\partial u}{\partial t} + u\frac{\partial u}{\partial x} + g_r \frac{\partial h}{\partial x} = 0. \tag{1.3}$$

In the above equations, u is the depth-averaged velocity in the x direction and h is the height of the current. To solve (1.2) and (1.3), one needs the constrained condition (or equivalently, the release condition at the current source [13]) given by

$$\int_0^{x_f} h(x,t)dx = Q_\alpha t^\alpha \quad (\text{or } uh|_{x=0} = \alpha Q_\alpha t^{\alpha-1}), \tag{1.4}$$

where x_f is the forefront position of the current head (see Fig. 1). This condition presents the conservation of current volume, where $Q_\alpha t^\alpha$ accounts for the volume of the gravity current per unit width. In (1.4), $\alpha=0$ corresponds to the "constant volume" current which can be generated by the instantaneous release of a given volume of fluid, and $\alpha=1$ corresponds to the "constant flux" current arising whenever a fluid discharges from a source of a constant inflow rate [10,13]. Another condition considered is the so-called front condition (1.1) at the current front in which the parameter β (or a frontal Froude number) is determined theoretically or experimentally as a prerequisite of the problem. Because of the use of β in (1.1), this unsteady approach was regarded to be nonclosed [7].

Slim and Huppert [12] argued that although the front condition (1.1) is not rigorously applicable on the unsteady motion of gravity current, it nevertheless can be used as "a guide" [12]. Klemp *et al.* [4] stressed in a more straightforward way that for the hyperbolic-type SWE, the use of the front condition at downstream is a "logical reconciliation" because the SWE do not take the influence of the ambient fluid into account but the front condition actually accounts for the force balance between the current buoyancy and the ambient resistance. In the present paper, we propose a novel approach so that this reconciliation can be avoided. We rederive the SWE by taking the ambient resistance into account and obtain the so-called modified shallow water equations (MSWE) in which the ambient resistance is accounted for by a nonlinear term in the equation. As a result, the use of the front condition becomes unnecessary. The highly nonlinear MSWE can be approximately solved by the perturbation method. The perturbation equations turn out to be singular; the gravity current is then divided into two parts so that the matched asymptotic expansion can be applied. One part is the far field away from the current head and the other part is the near field close to the current head. After matching the inner solutions of the near field and the outer solutions of the far field at intermediate region, the composite solutions are eventually obtained for the entire current. To validate the MSWE, we apply the new equations on two commonly discussed currents: the constant flux current ($\alpha=1$) and the constant volume current ($\alpha=0$). For both cases, we obtain the outer solutions which are the same as those of previous studies in which the conventional SWE were solved with the source and the front conditions. More interestingly, the parameter β of the front condition (1.1) becomes a part of the inner solutions, implying that the resistance from the ambient fluid considered in the front condition is now successfully included in the MSWE.

In this paper, we present the derivation of the MSWE in Sec. II, solve the MSWE for the constant flux current in Sec. III, and for the constant volume current in Sec. IV. In Sec. III, we also introduce the Chezy drag term into the MSWE to take the turbulent drag effect into account. Finally we discuss the results, and conclusions are drawn in Sec. V.

II. MODIFIED SHALLOW WATER EQUATIONS

Consider an inviscid gravity current (flow I) intruding into an inviscid, motionless, and unbounded ambient fluid (flow II), see Fig. 1. At the interface, it is assumed that neither surface tension nor mixing exists. The governing equations of the gravity current are

$$\frac{\partial u}{\partial x} + \frac{\partial v}{\partial y} + j\frac{u}{x} = 0, \tag{2.1a}$$

$$\frac{\partial u}{\partial t} + u\frac{\partial u}{\partial x} + v\frac{\partial u}{\partial y} = -\frac{1}{\rho}\frac{\partial P}{\partial x}, \tag{2.1b}$$

$$\frac{\partial v}{\partial t} + u\frac{\partial v}{\partial x} + v\frac{\partial v}{\partial y} = -\frac{1}{\rho}\frac{\partial P}{\partial y} - g, \tag{2.1c}$$

in which u and v are the velocity components in the x and y directions, respectively, $j=0$ accounts for the planar flow and $j=1$ for the axisymmetric flow, and P is the pressure inside the current. At a large time after release, the horizontal velocity and the length of the current are much larger than their vertical counterparts so that the horizontal velocity can be assumed to be uniform across the current depth due to the irrotationality of the flow, i.e., $u=u(x,t)$. As a result, (2.1a) can be simplified by integrating it across the current depth, yielding

$$\frac{\partial h}{\partial t} + \frac{\partial (uh)}{\partial x} + j\frac{uh}{x} = 0. \tag{2.2}$$

In deriving (2.2) we apply the condition $v|_{y=0}=0$ at the impermeable ground and the kinematic boundary condition $v|_{y=h}=\partial h/\partial t+u(\partial h/\partial x)$ at the interface. Due to the hydrostatic approximation that the acceleration in the y direction is neglected, (2.1c) can be reduced to

$$P(x,y,t) = P_i(x,t) + \rho g(h-y), \tag{2.3}$$

where P_i is the pressure at the interface. After applying (2.3) on (2.1b), we obtain the simplified horizontal momentum equation as

$$\frac{\partial u}{\partial t} + u\frac{\partial u}{\partial x} + g\frac{\partial h}{\partial x} = -\frac{1}{\rho}\frac{\partial P_i}{\partial x}. \tag{2.4}$$

To find P_i, we apply the unsteady Bernoulli's equation along the instant streamline emanating from the current surface (see Fig. 1) and obtain

$$P_i(x,t) = P_t - \rho_a g h - \frac{1}{2}\rho_a (\vec{V}_i)^2 - \rho_a \left.\frac{\partial \phi}{\partial t}\right|_{y=h(x,t)}, \tag{2.5}$$

in which $\vec{V}_i$ is the instant absolute velocity of the ambient fluid at the interface, ϕ the velocity potential defined by $\vec{V}=\nabla\phi$, and P_t is the total pressure of the ambient fluid far away from the current. Since the ambient flow is unbounded and motionless, P_t is considered as a constant. Consequently, (2.4) becomes

$$\frac{\partial u}{\partial t} + u\frac{\partial u}{\partial x} + g_r\frac{\partial h}{\partial x} = \frac{\gamma}{2}\frac{\partial (\vec{V}_i)^2}{\partial x} + \gamma\frac{\partial}{\partial x}\left[\left.\frac{\partial \phi}{\partial t}\right|_{y=h(x,t)}\right]. \tag{2.6}$$

The two terms on the right-hand side of (2.6) account for the dynamical pressure drag (or the form drag) applied on the current from the ambient fluid.

To solve (2.6) one needs to determine $\vec{V}_i$ and ϕ; both are functions of h and/or u. To do this, we first decompose $\vec{V}_i$ into the tangential velocity w_t and the normal velocity w_n. The w_n can be determined by the kinematic boundary condition

$$\frac{DF}{Dt} = \frac{\partial F}{\partial t} + \vec{V}_i \cdot \nabla F = \frac{\partial F}{\partial t} + |\nabla F| w_n = 0, \tag{2.7}$$

where $F=y-h(x,t)=0$, yielding

$$w_n = -\frac{1}{|\nabla F|}\frac{\partial F}{\partial t} = \frac{\partial h/\partial t}{\sqrt{1+(\partial h/\partial x)^2}}. \tag{2.8}$$

For the tangential velocity w_t, since the horizontal gradient of normal velocity is usually larger than that of tangential velocity at the current head, we accordingly assume that $\partial(w_n^2)/\partial x \gg \partial(w_t^2)/\partial x$ so that (2.6) is simplified into

$$\frac{\partial u}{\partial t} + u\frac{\partial u}{\partial x} + g_r\frac{\partial h}{\partial x} = \frac{\gamma}{2}\frac{\partial}{\partial x}\left[\frac{(\partial h/\partial t)^2}{1+(\partial h/\partial x)^2}\right] + \gamma\frac{\partial}{\partial x}\left[\left.\frac{\partial \phi}{\partial t}\right|_{y=h(x,t)}\right]. \tag{2.9}$$

It is noted that the assumption $\partial(w_n^2)/\partial x \gg \partial(w_t^2)/\partial x$ is supported by previous results (see, for example, Droegemeier and Wilhelmson [14] in which the streamline patterns of a thunderstorm current simulated numerically support this assumption fairly well) and the present results (as will be shown in Sec. III D that the present results are in good agreement with previous experimental data). By virtue of this assumption, the last term of (2.9) can be simplified further into

$$\frac{\partial}{\partial x}\left[\left.\frac{\partial \phi}{\partial t}\right|_{y=h(x,t)}\right] \approx -\frac{\partial}{\partial x}\left[\frac{(\partial h/\partial t)^2}{1+(\partial h/\partial x)^2}\right]. \tag{2.10}$$

The details of the derivation of (2.10) are shown in Appendix A. After substituting (2.10) into (2.9) and making the necessary arrangements, we obtain

$$\frac{\partial u}{\partial t} + u\frac{\partial u}{\partial x} + g_r\frac{\partial h}{\partial x} = -\frac{\gamma}{2}\frac{\partial}{\partial x}\left[\frac{(\partial h/\partial t)^2}{1+(\partial h/\partial x)^2}\right]. \tag{2.11}$$

Equations (2.2) and (2.11) are two simultaneous differential equations for u and h and shall be called the modified shallow-water equations (MSWE) afterward. The MSWE are valid for a two-dimensional planar ($j=0$) or axisymmetric ($j=1$) inviscid gravity current intruding beneath an inviscid quiescent unbounded ambient fluid. The specialty of the MSWE is that the resistance force in terms of the dynamic pressure [see (2.6)] is included in the equations so that the use of the front condition (1.1) becomes unnecessary. Note that as $\gamma \ll 1$ is considered, the dynamical pressure drag is negligible so that the MSWE are degenerated into the SWE. When $\gamma > 1$ is considered, the reduced gravity is negative and the equations are good for an upside-down gravity current [6,7,11], in which case the dynamical pressure drag becomes greater and predominates the motion of the current.

Since the MSWE are highly nonlinear, we employ the perturbation method to solve the equations approximately. In developing the perturbation equations, it is found that the small parameter ε multiplies with the term of the highest derivative, resulting in a singular perturbation problem. Accordingly, the method of matched asymptotic expansion is employed. The gravity current is therefore divided into two regions, the far field away from the current front and the near field close to the current front. The solutions of these two fields are then matched at the interface between these two fields.

We solve the MSWE for two commonly discussed currents, i.e., the constant flux current ($\alpha=1$) and the constant volume current ($\alpha=0$). Only the planar gravity current is considered because for the axisymmetric gravity current there is a singular point at $x=0$, which makes the highly nonlinear MSWE more difficult to be solved.

III. CONSTANT FLUX CURRENTS ($\alpha=1$)

For constant flux currents, the current flow will develop into a self-similar phase at a sufficiently long time after its release [9,12]. In such a phase, the flow becomes a long and narrow current and its velocity and height at the source become stable and approach to constant values u_0 and h_0, respectively. These conditions will be used in the far field analysis. In the following, we will first show the far field solution in Sec. III A and the inner solution in Sec. III B and then match the two solutions at the matching point in Sec. III C. Consequently, the complete composite solutions are obtained for the entire current, including the flow within the head. In Sec. III D we introduce the inviscid Chezy drag, or the turbulent drag [15], into the MSWE to account for the turbulent drag imposed on the current head and show that this viscous correction for the MSWE leads to a good agreement between the present results and the experimental data.

A. Far field solutions

At the far field away from the current head, we employ the following dimensionless outer variables

$$x' = \frac{x}{L}, \quad t' = \frac{u_0}{L}t, \quad u'(x',t') = \frac{u(x,t)}{u_0}, \quad h'(x',t') = \frac{h(x,t)}{h_0}, \tag{3.1}$$

to nondimensionalize (2.2) and (2.11), yielding

$$\frac{\partial h'}{\partial t'} + \frac{\partial (u'h')}{\partial x'} = 0, \tag{3.2a}$$

$$\frac{\partial u'}{\partial t'} + u'\frac{\partial u'}{\partial x'} + \frac{1}{\beta_0^2}\frac{\partial h'}{\partial x'} = -\varepsilon^2 \frac{\gamma}{2}\frac{\partial}{\partial x'}\left[\frac{(\partial h'/\partial t')^2}{1+(\varepsilon \partial h'/\partial x')^2}\right], \tag{3.2b}$$

where L is the total length of the current, $\varepsilon = h_0/L$, and $\beta_0 = u_0/\sqrt{g_r h_0}$ is the source Froude number. Because ε is a small parameter since $L \gg h_0$, (2.2a) and (2.2b) are singular. To solve these singular equations, we expand u' and h' into a power series of ε as follows:

$$u' = u'_{(0)} + \varepsilon u'_{(1)} + \ldots, \tag{3.3a}$$

$$h' = h'_{(0)} + \varepsilon h'_{(1)} + \ldots, \tag{3.3b}$$

where the subscript "(n)" denotes the nth-order term. These power series are substituted into (3.2a) and (3.2b), and the terms of the same order are collected to form the perturbation equations of each order. The leading order ($n=0$) equations are

$$\frac{\partial h'_{(0)}}{\partial t'} + \frac{\partial u'_{(0)} h'_{(0)}}{\partial x'} = 0, \tag{3.4a}$$

$$\frac{\partial u'_{(0)}}{\partial t'} + u'_{(0)}\frac{\partial u'_{(0)}}{\partial x'} + \frac{1}{\beta_0^2}\frac{\partial h'_{(0)}}{\partial x'} = 0, \tag{3.4b}$$

which are identical to the dimensionless form of the conventional SWE (1.1) and (1.2), implying that the dynamical pressure drag is negligible far away from the current head.

According to Gratton and Vigo [13], (3.4a) and (3.4b) admit a family of self-similar solutions to describe the intermediate asymptotic behavior of the gravity current, for which the precise initial conditions become irrelevant. By referring to the analysis of Gratton and Vigo as well as the boundary conditions at the source, we consider the similarity variables as

$$u'_{(0)}(x',t') = \tilde{u}(\eta), \quad h'_{(0)}(x',t') = \beta_0^2 \tilde{h}(\eta), \quad \eta = x'/t'. \tag{3.5}$$

With these variables, (3.4a) and (3.4b) become

$$\tilde{h}\frac{d\tilde{u}}{d\eta} + (\tilde{u}-\eta)\frac{d\tilde{h}}{d\eta} = 0, \tag{3.6a}$$

$$(\tilde{u}-\eta)\frac{d\tilde{u}}{d\eta} + \frac{d\tilde{h}}{d\eta} = 0. \tag{3.6b}$$

These two equations have trivial uniform solutions

$$\tilde{u} = B_1, \quad \tilde{h} = B_2, \tag{3.7}$$

in which B_1 and B_2 are integration constants to be determined by the boundary conditions at the current source. According to the phase-plane analysis of Gratton and Vigo [13], the uniform outer solution first occurs at the current source, where $u(0,t)=u_0$ and $h(0,t)=h_0$, or with the scaling (3.1) and (3.5), yielding $B_1=B_2=1$. To obtain the nontrivial solution of (3.6) requires that the coefficient determinant of (3.6a) and (3.6b) be zero, i.e.,

$$\begin{vmatrix} \tilde{h} & (\tilde{u}-\eta) \\ (\tilde{u}-\eta) & 1 \end{vmatrix} = 0, \tag{3.8}$$

or $\tilde{h}=(\tilde{u}-\eta)^2$. By substituting this into (3.6a) and (3.6b), we obtain

$$\tilde{u} = \frac{2}{3}\eta + C_1, \quad \tilde{h} = \left(C_1 - \frac{\eta}{3}\right)^2. \tag{3.9}$$

The integration constant C_1 cannot be determined until the matching with the inner solutions is accomplished.

By referring to the relations of (3.1) and (3.5), the trivial uniform solutions (3.7) can be rewritten in the original form as

$$u_{(0)}^{uni} = u_0, \quad h_{(0)}^{uni} = h_0, \tag{3.10}$$

and the nontrivial solutions (3.9) as

$$u_{(0)}^{ct} = \frac{2}{3}\frac{x}{t} + C_1 u_0, \quad h_{(0)}^{ct} = g_r^{-1}\left(C_1 u_0 - \frac{1}{3}\frac{x}{t}\right)^2, \tag{3.11}$$

where the superscripts "*uni*" and "*ct*" denote the uniform solution and the nontrivial solution, respectively. Mathematically, both trivial and nontrivial solutions may exist simultaneously. According to Gratton and Vigo [13], the true outer solutions are constructed by matching uniform solutions with nontrivial solutions (see Fig. 2). The uniform solution (3.10)

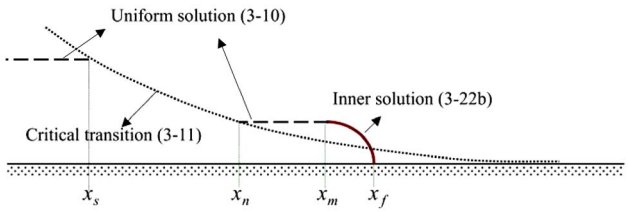

FIG. 2. (Color online) The conjugate point between uniform solution (3.10) and critical transition (3.11) is denoted by x_s, and the conjugate point between near field and far field is denoted by x_n. The margin point of the near field is x_m.

first appears at the source, and the nontrivial solution (3.11) subsequently joins to describe the falling behavior of the current. Gratton and Vigo called (3.11) "the critical transition" because it describes the transition from upstream to downstream conditions. To construct the outer solutions, we assume that the first conjugate point locates at $x=x_s$ (see Fig. 2), where the velocity and the height are continuous, i.e.,

$$u_{(0)}^{uni}|_{x=x_s} = u_{(0)}^{ct}|_{x=x_s}, \quad h_{(0)}^{uni}|_{x=x_s} = h_{(0)}^{ct}|_{x=x_s}, \tag{3.12}$$

which account for two simultaneous equations for C_1 and x_s.

Since (3.10) is linear and (3.11) is binomial, there are two possible distinctive solutions (see Fig. 3). One solution accounts for the combination of the uniform solution and the descending part of (3.11), describing the falling behavior of the gravity current, i.e.,

$$C_1 = \frac{\beta_0 + 2}{3\beta_0}, \quad x_s = \left(\frac{\beta_0 - 1}{\beta_0}\right) u_0 t. \tag{3.13}$$

Another solution accounts for the combination of the uniform solution and the ascending part of (3.11), describing the rising behavior of the gravity current, i.e.,

$$C_1 = \frac{\beta_0 - 2}{3\beta_0}, \quad x_s = \left(\frac{\beta_0 + 1}{\beta_0}\right) u_0 t. \tag{3.14}$$

We show in Appendix B that (3.14) is physically unreasonable and therefore only the descending part solution (3.13) will be considered in the following analysis.

Consequently, the second uniform solutions join the critical transition at the second conjugate point x_n (see Fig. 2), where the velocity and the height are continuous, i.e.,

$$\frac{2}{3}\frac{x_n}{t} + C_1 u_0 = u_{(0)}|_{x=x_n}, \tag{3.15a}$$

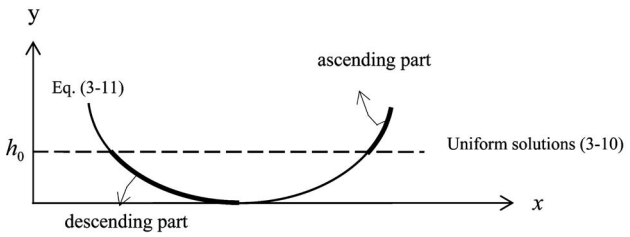

FIG. 3. Illustration of the conjugation of the uniform solutions (3.10) and the critical transition (3.11).

$$g_r^{-1}\left[C_1 u_0 - \frac{1}{3}\frac{x_n}{t}\right]^2 = h_{(0)}|_{x=x_n}. \tag{3.15b}$$

Note that $x_n, u_{(0)}|_{x=x_n}$ and $h_{(0)}|_{x=x_n}$ cannot be determined until the matching with the inner solution is accomplished.

B. The near field solution

In the near field we assume $(x_f - x_m)$ to be the characteristic length L_C, where x_f is the foremost point of the gravity current and x_m the margin point of the near field (see Fig. 2). In the near field the characteristic length L_C shall satisfy the condition $h_0/L_C = O(1)$ or $L_C/L = \varepsilon$ [16]. The dimensionless inner variables are then given by

$$X \equiv \frac{x - x_m(t)}{L_C} = \frac{x' - x_m'(t')}{\varepsilon}, \tag{3.16a}$$

$$U(X,t') \equiv \frac{u}{u_0} = u'(x',t'), \tag{3.16b}$$

$$H(X,t') \equiv \frac{h}{h_0} = h'(x',t'). \tag{3.16c}$$

Equations (3.2a) and (3.2b) are nondimensionalized by these inner variables and become

$$\frac{\partial H}{\partial t'} - \frac{1}{\varepsilon}\frac{dx_m'}{dt'}\frac{\partial H}{\partial X} + \frac{1}{\varepsilon}\frac{\partial (UH)}{\partial X} = 0, \tag{3.17a}$$

$$\frac{\partial U}{\partial t'} - \frac{1}{\varepsilon}\frac{dx_m'}{dt'}\frac{\partial U}{\partial X} + \frac{U}{\varepsilon}\frac{\partial U}{\partial X} + \frac{1}{\varepsilon\beta_0^2}\frac{\partial H}{\partial X} = -\frac{\gamma}{2\varepsilon}\frac{\partial}{\partial X}\left[\frac{\left(\varepsilon\frac{\partial H}{\partial t'} - \frac{dx_m'}{dt'}\frac{\partial H}{\partial X}\right)^2}{1 + \left(\frac{\partial H}{\partial X}\right)^2}\right]. \tag{3.17b}$$

Again, the perturbation method is employed to solve these equations. After substituting the power series of H and U like (3.3) into these two equations and collecting the terms of the same order to form perturbation equations of each order, we obtain the leading order equations as

$$-\frac{dx_m'}{dt'}\frac{\partial H_{(0)}}{\partial X} + \frac{\partial U_{(0)} H_{(0)}}{\partial X} = 0, \tag{3.18a}$$

$$-\frac{dx_m'}{dt'}\frac{\partial U_{(0)}}{\partial X} + U_{(0)}\frac{\partial U_{(0)}}{\partial X} + \frac{1}{\beta_0^2}\frac{\partial H_{(0)}}{\partial X} = -\frac{\gamma}{2}\left(\frac{dx_m'}{dt'}\right)^2 \frac{\partial}{\partial X}\left[\frac{(\partial H_{(0)}/\partial X)^2}{1 + (\partial H_{(0)}/\partial X)^2}\right], \tag{3.18b}$$

in which $U_{(0)}$, $u_{f_{(0)}}'$, and $H_{(0)}$ are the leading order terms of the power series of U, u_f', and H, respectively. To solve these two equations, we integrate (3.18a) once over X and obtain

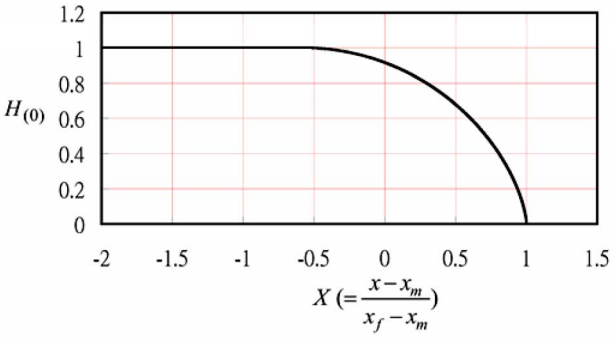

FIG. 4. (Color online) The height profile is obtained by computing the inner equation (3.21) numerically. The solutions correspond to $\gamma\beta_0^2 U_{(0)}^2=2$, and the boundary conditions used are $H_{(0)}=0$ and $\partial H_{(0)}/\partial X=-\infty$ at $X=1$.

$$-\frac{dx_m'}{dt'}H_{(0)}+U_{(0)}H_{(0)}=B_3(t). \tag{3.19}$$

The integration function B_3 shall be zero to satisfy that $H_{(0)}$ be zero when the current surface touches the horizontal bed. As a result,

$$U_{(0)}=\frac{dx_m'}{dt'}, \tag{3.20}$$

whose value is to be determined by matching with the outer solutions of the far field. Note that since x_m' depends on t' but not on X, $U_{(0)}$ shall be uniform so that $u_{f_{(0)}}'=U_{(0)}$ and the first two terms on the left-hand side of (3.18b) vanish. This gives

$$\frac{1}{\beta_0^2}\frac{\partial H_{(0)}}{\partial X}=-\frac{\gamma}{2}U_{(0)}^2\frac{\partial}{\partial X}\left[\frac{(\partial H_{(0)}/\partial X)^2}{1+(\partial H_{(0)}/\partial X)^2}\right]. \tag{3.21}$$

This equation balances the forces between the static pressure within the current head and the dynamical pressure drag applied on the current head. A typical numerical solution of (3.21) in terms of the profile of current head is shown in Fig. 4. The present inner solution (3.21) gives a current head having a smooth profile, being more physically reasonable than those obtained by solving the conventional SWE (see, for example, Fig. 13 of Klemp *et al.* [4] or Fig. 9 of Gratton and Vigo [13] in which the current heads appeared as a vertically cut front). Referring to (3.16), the inner solutions in terms of the original variables are

$$u_{(0)}^{inner}=u_{f_{(0)}}=\frac{dx_m}{dt}, \tag{3.22a}$$

$$h_{(0)}^{inner}=h_0H_{(0)}(X,t'). \tag{3.22b}$$

Note again that the function $H_{(0)}$ is obtained by solving (3.21) numerically.

C. Asymptotically matched solution

For constant flux currents, the matching requires that inner solutions $u_{(0)}^{inner}$ and $h_{(0)}^{inner}$ at $X=-\infty$ attach to the uniform outer solutions $u_{(0)}^{ct}|_{x=x_n}$ and $h_{(0)}^{ct}|_{x=x_n}$, respectively. However, since no explicit analytical inner solution can be used directly to match the outer solution, a further simplification is necessary. To do this, we first integrate (3.21) once and obtain

$$H_{(0)}=-\frac{\gamma\beta_0^2}{2}U_{(0)}^2\left[\frac{\left(\frac{\partial H_{(0)}}{\partial X}\right)^2}{1+(\partial H_{(0)}/\partial X)^2}\right]+f(t'), \tag{3.23}$$

where $f(t')$ is the integration function. Since the inner solution must match the uniform part of the outer solution, the slope of the current profile shall be zero when $H_{(0)}=h'_{(0)}|_{x=x_n}$ (see Fig. 2). Therefore, (3.23) gives

$$f(t')=h'_{(0)}|_{x=x_n}. \tag{3.24}$$

Another condition required to solve (3.21) analytically is that $\partial H_{(0)}/\partial X=-\tan\theta_c$, which shall be satisfied at the contact point and θ_c is the contact angle. After substituting (3.24) as well as this condition into (3.23), we obtain

$$\frac{2\,h'_{(0)}|_{x=x_n}}{\gamma U_{(0)}^2\beta_0^2}=\frac{\tan^2\theta_c}{1+\tan^2\theta_c}\equiv\Lambda(\theta_c). \tag{3.25}$$

Equation (3.25) can be rewritten in terms of the original variables, yielding

$$u_{f_{(0)}}=\sqrt{\frac{2}{\gamma\Lambda(\theta_c)}g_r\,h_{(0)}|_{x=x_n}}. \tag{3.26}$$

Note that (3.26) turns out to be equivalent to the front condition (1.6), provided that

$$\beta=\sqrt{\frac{2}{\gamma\Lambda(\theta_c)}}, \tag{3.27}$$

where β is a function of both the density ratio γ and the contact angle θ_c. It is interesting to note that for a contact angle $\theta_c\approx 90°$, (3.25) gives $\Lambda\approx 1$ and $\beta\approx\sqrt{2/\gamma}$, which is exactly the same with the result obtained by the steady-state approach [see (1.1)], suggesting that $\theta_c=90°$ be a proper physical condition for the present approach. In fact, this inference will be confirmed in Sec. III D, where we introduce the inviscid Chezy drag into the MSWE so that the present theoretical results can compare nicely with the experimental data.

After obtaining (3.26), we are ready to get the composite solutions as follows. We use (3.26) to combine (3.15a) and (3.15b) to determine the second conjugate point as

$$x_n=3\frac{(\beta-1)}{(\beta+2)}C_1u_0t, \tag{3.28}$$

in which β is given in (3.27). With this x_n, (3.15a) and (3.15b) become

$$u_{f_{(0)}}=\frac{3\beta}{\beta+2}C_1u_0, \tag{3.29}$$

$$h_{(0)}|_{x=x_n} = \left(\frac{3C_1}{\beta+2}\right)^2 \frac{u_0^2}{g_r}. \tag{3.30}$$

Since $u_{f(0)}=U_{(0)}=dx_m/dt$, we can integrate (3.29) with respect to t to obtain

$$x_m = \frac{3\beta}{\beta+2} C_1 u_0 t. \tag{3.31}$$

So far, we have obtained the leading order solutions for the composite gravity current of a constant flux, which are summarized in the following:

$$u_{(0)} = \begin{cases} u_0, & 0 \leqslant x \leqslant x_s \text{ (current source)}, \\ \dfrac{2}{3}\dfrac{x}{t} + C_1 u_0, & x_s \leqslant x \leqslant x_n \text{ (descending transition)}, \\ \dfrac{3\beta}{\beta+2} C_1 u_0, & x_n \leqslant x \leqslant x_f \text{ (current head)}, \end{cases} \tag{3.32}$$

$$h_{(0)} = \begin{cases} h_0, & 0 \leqslant x \leqslant x_s \text{ (current source)}, \\ g_r^{-1}[C_1 u_0 - x/3t]^2, & x_s \leqslant x \leqslant x_n \text{ (descending transition)}, \\ h_0 H_{(0)}, & x_n \leqslant x \leqslant x_f \text{ (current head)}, \end{cases} \tag{3.33}$$

where β, x_s, and x_n are given in (3.27), (3.13), and (3.28), respectively, and $H_{(0)}$ is the solution given by (3.21). To exemplify the results, we show in Fig. 5 the solutions of (3.32) and (3.33) for $\beta_0=1.8$ with six different γ (curves a–f).

Note that the above solutions are valid only for $\beta_0 \leqslant \beta$ (see the discussion in Appendix B). According to Gratton and Vigo [13], $\beta_0 > \beta$ leads to a discontinuous hydraulic jump at an intermediate region of the current. To construct the discontinuous solutions, the jump conditions must be used at some intermediate region of the current to match the two uniform outer solutions. For curiosity, a typical discontinuous solution is also given in Fig. 5, see curve (g). Note that curve (a), corresponding to the limited solution for non-Boussinesq gravity currents ($\gamma \approx 0$), accounts for the classical solution of the dam-break problem, in which no ambient resistance is imposed on the current and the head vanishes.

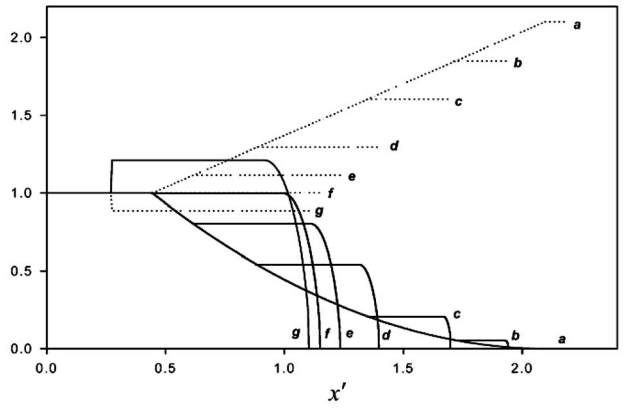

FIG. 5. Leading order solutions of constant flux currents ($\alpha=1$) at $t'=1$. The solid lines account for dimensionless depth profiles, and the dotted lines for dimensionless velocities. The solutions correspond to $\beta_0=1.8$, (a) $\gamma=0$ ($\beta \approx \infty$), (b) $\gamma=0.01$ ($\beta \approx 14$), (c) $\gamma=0.05$ ($\beta \approx 6.3$), (d) $\gamma=0.2$ ($\beta \approx 3.16$), (e) $\gamma=0.4$ ($\beta \approx 2.24$), (f) $\gamma=0.617$ ($\beta \approx 1.8$), and (g) $\gamma=0.95$ ($\beta \approx 1.45$).

Obviously, as shown by curve (g), only Boussinesq gravity currents ($\gamma \approx 1$) can lead to $\beta_0 > \beta$ as well as a hydraulic jump.

D. Viscous correction of MSWE

To consider the viscous effect on gravity currents, one may follow the procedure of Sec. II to derive the viscous MSWE when the viscous terms are included in (2.1), but unfortunately, an accurate and compact expression of the shear stress cannot be acquired due to the complicated flow motion both at the interface and on the bottom surface and the resultant equations can be too complicated to be solved analytically. To consider the viscous effect on the gravity current in a feasible way, Hogg and Pritchard [15] proposed a semiempirical relation or the so-called inviscid Chezy drag $\tau=\rho C_D u^2$ for the large-scale turbulent gravity currents, where the turbulent drag coefficient C_D frequently falls within the range 0.01–0.001. To examine the viscous correction for the inviscid MSWE, we introduce the Chezy drag into the MSWE and obtain

$$\frac{\partial u}{\partial t} + u\frac{\partial u}{\partial x} + g_r \frac{\partial h}{\partial x} = -\frac{\gamma}{2}\frac{\partial}{\partial x}\left[\frac{(\partial h/\partial t)^2}{1+(\partial h/\partial x)^2}\right] - \frac{C_D u^2}{h}. \tag{3.34}$$

We solve (3.34) for constant flux currents with the same procedure as shown in Sec. III. For the analysis of the far field, we employ (3.1) to nondimensionalize outer equations, yielding

$$\frac{\partial u'}{\partial t'} + u'\frac{\partial u'}{\partial x'} + \frac{1}{\beta_0^2}\frac{\partial h'}{\partial x'} = -\varepsilon^2 \frac{\gamma}{2}\frac{\partial}{\partial x'}\left[\frac{(\partial h'/\partial t')^2}{1+(\varepsilon \partial h'/\partial x')^2}\right] - \frac{C_D u'^2}{\varepsilon h'}. \tag{3.35}$$

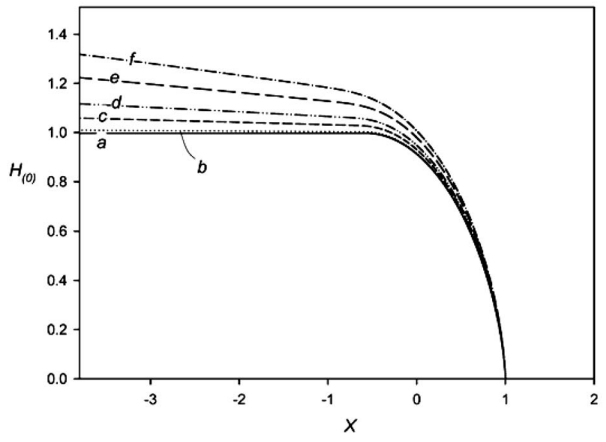

FIG. 6. Height profiles within the near field, obtained by solving (3.36) numerically together with the conditions (3.37) for $\gamma=1$, $\beta_0 U_{(0)}=\sqrt{2}$, and six turbulent drag coefficients C_D: (a) 0.0001, (b) 0.001, (c) 0.005, (d) 0.01, (e) 0.02, and (f) 0.03.

Note that if the turbulent drag coefficient is small, say $C_D \leqslant O(\varepsilon^2)$, the Chezy drag term of (3.35) can be neglected. In such a case the outer equations are the same with (3.4a) and (3.4b) and their outer solutions are (3.10) and (3.11). But for a larger drag coefficient, say $C_D=O(\varepsilon)$, the Chezy drag term is no longer negligible so that (3.35) cannot be solved analytically. Nonetheless, since C_D frequently falls within the range 0.01–0.001, being of an order of $O(\varepsilon^2)$ or $O(\varepsilon^3)$, the outer solution (3.10) and (3.11) can therefore be applied for the present case.

For the analysis of the near field, the effects of the turbulent drag are significant because the Chezy drag term becomes very large in the vicinity of the contact point (where $h \to 0$). After employing the inner variables (3.16) to nondimensionalize the inner equations and applying the perturbation procedure on the dimensionless equations, the leading-order inner equation is obtained as

$$\frac{1}{\beta_0^2}\frac{\partial H_{(0)}}{\partial X} = -\frac{\gamma}{2}U_{(0)}^2\frac{\partial}{\partial X}\left[\frac{(\partial H_{(0)}/\partial X)^2}{1+(\partial H_{(0)}/\partial X)^2}\right] - C_D\frac{U_{(0)}^2}{H_{(0)}}. \tag{3.36}$$

It is found from (3.36) that $H_{(0)} \to 0$ gives $U_{(0)}^2/H_{(0)}=\infty$, so that $\partial H_{(0)}/\partial X=-\infty$. Accordingly, we solve (3.36) numerically together with the boundary conditions

$$H_{(0)}=0 \text{ and } \partial H_{(0)}/\partial X=-\infty \text{ at } X=1. \tag{3.37}$$

The results for $\gamma=1$, $\beta_0 U_{(0)}=\sqrt{2}$, and six different C_D are shown in Fig. 6.

From Fig. 6 one can see that a larger turbulent drag gives a bigger current head with a higher h_f, which in turn leads to a smaller β according to the relation $u_f=\beta\sqrt{g_r h_f}$, given that u_f remains the same. This relation also leads to $\beta_1/\beta_2=\sqrt{h_{f2}/h_{f1}}$. Based on this relation as well as the results of Fig. 6, we can estimate the value of β for different C_D as follows. For example, for $C_D=0.03$ (see curve f) the height $H_{(0)}|_{X=-4}$ (assumed to account for the height of the current head h_f) is about 1.3 times that of $C_D=0.0001$, which corresponds to the inviscid gravity current having $\beta=\sqrt{2}$ for $\gamma=1$ [17]. So β for $\gamma=1$ and $C_D=0.03$ is calculated by the relation $\beta=\sqrt{2}\times\sqrt{1/1.3}=1.24$, which is close to the experimental value 1.19 obtained by Simpson and Britter [18]. With the same procedure, we also estimate other possible β for different γ and C_D and obtain the results shown in Fig. 7. In comparison with the experimental data of Groebelbauer *et al.* [2], we see that, clearly, the curve of $C_D=0.03$ fits the experimental data better than the inviscid case ($\beta=\sqrt{2/\gamma}$), and this trend becomes more evident for the currents having a smaller γ. This leads to a conclusion that for Boussinesq currents having $\gamma \approx 1$, the inviscid MSWE gives a result comparing fairly well with the experimental data. For non-Boussinesq currents having a small γ (such as the dam-break case), the inviscid form drag becomes insignificant and the turbulent drag effect predominates the resistance. Therefore the MSWE shall include the Chezy drag term to account for viscous effect.

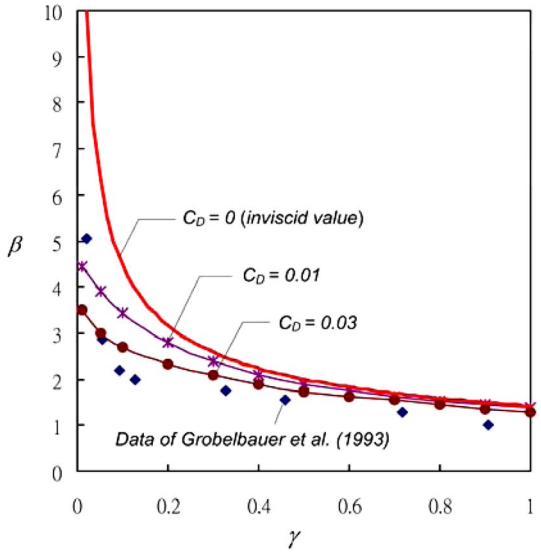

FIG. 7. (Color online) Estimation of values on β from numerical solutions of (3.36). The plot shows that a larger C_D gives a value of β closer to experimental data.

IV. CONSTANT VOLUME CURRENTS ($\alpha=0$)

The constant volume current can be generated from the sudden release of a fixed volume of a denser fluid into an infinite lighter ambient fluid, such as the dam-break problem, see Fig. 8 [19]. The current starts from an initial (slumping) phase, wherein a return bore propagates backward to upstream and a nose moves forward to downstream with a virtually constant speed. When the return bore touches the back wall, a reflected bore is formed and then propagates toward the current front. Once the reflected bore catches up with the current front, the current falls into the self-similar phase [20]. In this section we will develop the approximate solutions at both the initial phase and the self-similar phase.

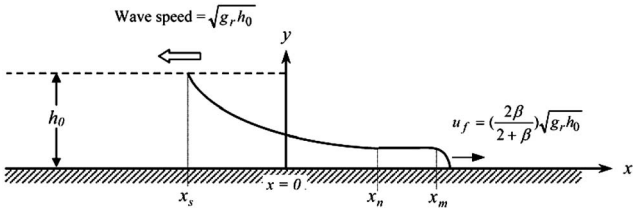

FIG. 8. Initial stage of the constant volume current. A backward wave propagating toward upstream with a constant wave speed $\sqrt{g_r h_0}$ is shown. The front head also moves at a constant speed, which is in terms of β.

A. The initial phase solution

At the initial phase, since the boundary conditions at the source are $u=0$ and $h=h_0$, the dimensionless outer variables can be chosen as

$$x' = \frac{x}{L}, \quad t' = \frac{\sqrt{g_r h_0}}{L}t, \quad u'(x',t') = \frac{u(x,t)}{\sqrt{g_r h_0}}, \tag{4.1}$$

$$h'(x',t') = \frac{h(x,t)}{h_0},$$

in which $\sqrt{g_r h_0}$ is chosen as the characteristic velocity. By using these outer variables, (2.2) and (2.11) are nondimensionalized into

$$\frac{\partial h'}{\partial t'} + \frac{\partial (u'h')}{\partial x'} = 0, \tag{4.2a}$$

$$\frac{\partial u'}{\partial t'} + u'\frac{\partial u'}{\partial x'} + \frac{\partial h'}{\partial x'} = \varepsilon^2 \frac{\gamma}{2}\frac{\partial}{\partial x'}\left[\frac{(\partial h'/\partial t')^2}{1+(\varepsilon \partial h'/\partial x')^2}\right]. \tag{4.2b}$$

After applying the same perturbation procedure as that of Sec., III, the leading order outer equations are obtained as

$$\frac{\partial h'_{(0)}}{\partial t'} + \frac{\partial u'_{(0)}h'_{(0)}}{\partial x'} = 0, \tag{4.3a}$$

$$\frac{\partial u'_{(0)}}{\partial t'} + u'_{(0)}\frac{\partial u'_{(0)}}{\partial x'} + \frac{\partial h'_{(0)}}{\partial x'} = 0. \tag{4.3b}$$

It is seen that the outer equations turn out to be identical with the conventional SWE. To solve these two equations we employ the similarity variables

$$u'_{(0)}(x',t') = \tilde{u}(\eta), \quad h'_{(0)}(x',t') = \tilde{h}(\eta), \quad \eta = x'/t', \tag{4.4}$$

to transform (4.3a) and (4.3b) into the same ordinary differential equations as (3.6a) and (3.6b) and, accordingly, the same similarity solutions as (3.7) and (3.9) are obtained. After applying the initial conditions, the uniform solutions (3.7) become $u_{(0)}^{uni}=0$ and $h_{(0)}^{uni}=h_0$, and the critical transition solutions are of the same form as (3.11). We assume again that the uniform solutions join the critical transition at $x=x_s$ (see Fig. 8), resulting in

$$0 = \frac{2}{3}\frac{x_s}{t} + C_2\sqrt{g_r h_0}, \tag{4.5}$$

$$h_0 = g_r^{-1}\left(C_2\sqrt{g_r h_0} - \frac{1}{3}\frac{x_s}{t}\right)^2. \tag{4.6}$$

As done in Sec. III A, matching at $x=x_s$ leads to two solution groups of C_2 and x_s, of which the only physically reasonable solutions are those matching the descending part of (3.11). They are

$$C_2 = \frac{2}{3} \quad \text{and } x_s = -\sqrt{g_r h_0}t. \tag{4.7}$$

For the inner solutions of the near field, we repeat the analysis of Sec. III C and obtain the same equations as well as the same solutions (3.26) and (3.27). This implies that the inner solutions are independent of the release conditions at the current source, which explains why the front condition can always be used single handedly for arbitrary release conditions. Again, we assume that the critical transition joins the second uniform solutions at $x=x_n$, resulting in

$$\frac{2}{3}\frac{x_n}{t} + C_2\sqrt{g_r h_0} = u_{f_{(0)}}, \tag{4.8}$$

$$g_r^{-1}\left(C_2\sqrt{g_r h_0} - \frac{1}{3}\frac{x_n}{t}\right)^2 = h_{(0)}|_{x=x_n}. \tag{4.9}$$

By considering (3.26) and (3.27), the above equations can be combined so that x_n can be determined as

$$x_n = \frac{2\beta-2}{2+\beta}\sqrt{g_r h_0}t \quad \text{or } x_n = \frac{-2\beta-2}{2-\beta}\sqrt{g_r h_0}t. \tag{4.10}$$

The second part of (4.10) is physically unreasonable because it gives $x_n<x_s$. Therefore, we substitute the first part of (4.10) into (4.8) and (4.9) and obtain

$$u_{f_{(0)}} = \frac{2\beta}{\beta+2}\sqrt{g_r h_0}, \quad h_{(0)}|_{x=x_n} = \left(\frac{2}{\beta+2}\right)^2 h_0. \tag{4.11}$$

Note that (4.11) is identical with the solution of Gratton and Vigo [13], although these two approaches are different in three aspects: (a) Gratton and Vigo considered the front condition (1.6) to account for the resistance force from the ambient fluid, while in the present study the resistance force is included in the governing equation (2.11). (b) The present approach provides a solution with a smooth profile of the current head, while that of Gratton and Vigo gave a vertically cut front. (c) In the present approach β is part of the solution, while β (or k) must be given as a prerequisite in Gratton and Vigo.

B. The self-similar phase solution

When the flow reaches the self-similar phase, its solution will no longer relate to the initial conditions. Hence, we consider the dimensionless outer variables

$$x' = \frac{x}{L}, \quad t' = \frac{u_0}{L}t, \quad u' = \frac{u}{u_0}, \quad h' = \frac{h}{h_0}, \tag{4.12}$$

in which the characteristic scales are $h_0=\sqrt{Q_0}$ and $u_0=Q_0^{1/4}g_r^{1/2}$, where Q_0 is the volume of the current per unit width [see (1.3)]. By nondimensionalizing the MSWE with these outer variables and applying the same perturbation procedure, we obtain the same leading order outer equations as (4.3a) and (4.3b). To catch the characteristics that the height of the current at the source decays with time, we follow Grundy and Rottman's approach [5] using the similarity variables

$$\eta = \frac{x'}{t'^{2/3}}, \quad u'_{(0)}(x',t') = t'^{-1/3}\tilde{u}(\eta), \quad h'_{(0)}(x',t') = t'^{-2/3}\tilde{h}(\eta), \tag{4.13}$$

to transform (4.3a) and (4.3b) into

$$-\frac{2}{3}\frac{d(\eta\tilde{h})}{d\eta} + \frac{d(\tilde{u}\tilde{h})}{d\eta} = 0, \tag{4.14a}$$

$$-\frac{1}{3}\tilde{u} - \frac{2}{3}\eta\frac{d\tilde{u}}{d\eta} + \tilde{u}\frac{d\tilde{u}}{d\eta} + \frac{d\tilde{h}}{d\eta} = 0. \tag{4.14b}$$

The above equations have a trivial "zero" solution, $\tilde{u}=\tilde{h}=0$, describing the dry region near the source [13]. Nevertheless, they also have a nontrivial solution to be derived in the following. We first integrate (4.14a) once, yielding

$$\left(-\frac{2}{3}\eta + \tilde{u}\right)\tilde{h} = B_4. \tag{4.15}$$

The integration constant B_4 is determined to be zero by the conditions that the velocity at the source is zero and the depth is finite as well as decays with time, so that (4.15) gives

$$\tilde{u} = 2\eta/3. \tag{4.16}$$

After substituting (4.16) into (4.14b) and integrating the resultant equation once, we obtain

$$\tilde{h}(\eta) = \frac{1}{9}\eta^2 + K', \tag{4.17}$$

where K' is an integration constant. Note that the nontrivial solutions (4.16) and (4.17) had been obtained by Hoult [7]. We rewrite these solutions in terms of the original variables as

$$u_{(0)}^{outer} = \frac{2}{3}\frac{x}{t}, \tag{4.18a}$$

$$h_{(0)}^{outer} = \frac{1}{9g_r}\left(\frac{x}{t}\right)^2 + Kt^{-(2/3)}, \tag{4.18b}$$

where the constant $K=(h_0^2L^2/g_r)^{1/3}K'$ is to be determined later. The continuous conditions at the matching point x_n are given by

$$u_{(0)}^{outer}|_{x=x_n} = \frac{2}{3}\frac{x_n}{t} = u_{(0)}^{inner}|_{X\to-\infty} = u_{f_{(0)}}, \tag{4.19a}$$

$$h_{(0)}^{outer}|_{x=x_n} = \frac{1}{9g_r}\left(\frac{x_n}{t}\right)^2 + Kt^{-(2/3)} = h_{(0)}^{inner}|_{X\to-\infty} = h_{(0)}|_{x=x_n}. \tag{4.19b}$$

Due to the independence of the inner solutions, we can match the outer solutions by substituting (3.26) and (3.27) into (4.19a) and (4.19b), respectively, and obtain

$$x_n = 3\beta\sqrt{\frac{Kg_r}{4-\beta^2}}t^{2/3}, \tag{4.20}$$

which is then substituted into (4.19a) and (4.19b) to obtain

$$u_{f(0)} = 2\beta\sqrt{\frac{Kg_r}{4-\beta^2}}t^{-(1/3)}, \quad h_{(0)}|_{x=x_n} = \left(\frac{4}{4-\beta^2}\right)Kt^{-(2/3)}. \tag{4.21}$$

Because $u_{f_{(0)}}=dx_m/dt$, we can integrate the above equation to yield

$$x_m = 3\beta\sqrt{\frac{Kg_r}{4-\beta^2}}t^{2/3}. \tag{4.22}$$

Note that (4.20) is identical with (4.22), or $x_n=x_m$, implying that the conjugate point is exactly the starting point of near field. We summarize the composite solution as follows:

$$u(x,t) = \begin{cases} \dfrac{2}{3}\dfrac{x}{t}, & 0 \le x < x_n, \\ 2\beta\sqrt{\dfrac{Kg_r}{4-\beta^2}}t^{-(1/3)}, & x_n \le x \le x_f, \end{cases} \tag{4.23}$$

$$h(x,t) = \begin{cases} \dfrac{1}{9g_r}\left(\dfrac{x}{t}\right)^2 + Kt^{-(2/3)}, & 0 \le x \le x_n, \\ h_0H_{(0)}, & x_n \le x \le x_f. \end{cases} \tag{4.24}$$

The parameters K and x_f remain to be determined. Note that there is no need to calculate x_f because, according to Mei [16], the value of x_f is proportional to the small parameter ε and therefore shall be a small value. The parameter K can be determined by considering the conservation of volume

$$\int_0^{x_m} h_{(0)}^{outer}dx + \int_{x_m}^{x_f} h_{(0)}^{inner}dx = Q_0. \tag{4.25}$$

However, in (4.25) $h_{(0)}^{inner}$ is a numerical solution of (3.21) so that an analytical solution of (4.25) is not available. A further simplification is therefore necessary. In doing so, we express the volume per unit width of the current head as $V_H(t)$ so that (4.25) is rewritten as

$$\int_0^{x_m} h_{(0)}^{outer}dx = Q_0 - V_H(t) \equiv V_0(t). \tag{4.26}$$

By substituting (4.18b) and (4.22) into (4.26), we obtain

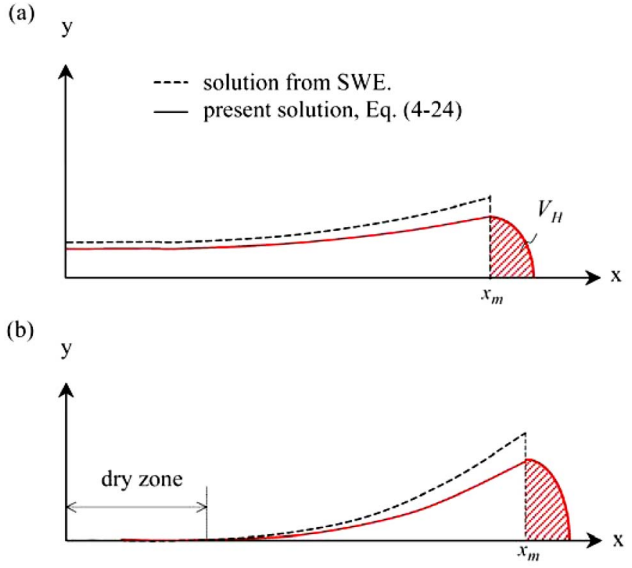

FIG. 9. (Color online) Comparison between the solution in terms of the current profile, obtained by solving the convectional SWE and the present solution obtained by solving the MSWE for the constant-volume case: (a) $\beta<2$; (b) $\beta\geqslant 2$.

$$K=\frac{4-\beta^2}{(12\beta-2\beta^3)^{2/3}}V_0(t)^{2/3}g_r^{-1/3}. \tag{4.27}$$

Since K is a constant, $V_0(t)$ shall be a constant too, implying that the volume of the current head $V_H(t)$ shall also be a constant. By virtue of this implication, the constant K is of the same form as (4.27) when $V_0(t)$ is replaced by $V_0=(Q_0-V_H)$, which is a constant. Eventually, by substituting this V_0 into (4.21) we obtain the height and speed at the current front as

$$h_{(0)}|_{x=x_n}=\frac{4}{(12\beta-2\beta^3)^{2/3}}V_0^{2/3}g_r^{-1/3}t^{-2/3}, \tag{4.28}$$

$$u_{f(0)}=\left(\frac{4\beta^2}{6-\beta^2}V_0g_r\right)^{1/3}t^{-1/3}. \tag{4.29}$$

These solutions are the same as previous solutions [5–13], as long as V_0 is replaced by Q_0, implying that the volume of the current head V_H was neglected by those studies. However, as shown in Fig. 9(a), V_H accounts explicitly for a part of the total volume of the current and shall not be neglected. Note also that the solutions (4.28) and (4.29) are valid only for $\beta<2$, since we have assumed there is no dry region at the source [13]. For $\beta\geqslant 2$, a dry zone appears at the source so that the zero solution accounts for the current at the source and joins with the nontrivial solutions (4.18a) and (4.18b) at the point where the depth is zero. For such a case, we can apply the same solution procedure and obtain the results consistent with those of Gratton and Vigo [13], as shown in Fig. 9(b).

V. DISCUSSION AND CONCLUSIONS

We rederive the shallow water equations for inviscid gravity currents of arbitrary density ratio by taking the ambient resistance into account and end up with the modified shallow water equations (2.2) and (2.11), in which the ambient resistance is accounted for by the nonlinear term on the right-hand side of (2.11). These highly nonlinear partial differential equations are solved by perturbation method approximately to the leading order. Since the resultant perturbation equations are singular, the gravity current is divided into the inner region near the current head and the outer region away from the current head so that the matched asymptotic expansion procedure can be applied. The outer equations are solved by similarity transformations while, unfortunately, the inner equations can only be solved numerically. Since the numerical inner solutions cannot be used to match with the analytical outer solutions, a further simplification is therefore applied so that the inner solution can be obtained in an analytical form; then the two solutions eventually can be matched at the intermediate region to obtain the composite solutions for the entire current. The MSWE are applied to the two commonly investigated cases, the constant flux ($\alpha=1$) and the constant volume ($\alpha=0$) gravity currents, and the solutions are summarized in Table I. Although the present solutions only approximate to the leading order, a solution of high-order approximation is unnecessary because the nonlinear term of (3.2b) is of an order of ε^2 so that higher order terms only make an insignificant contribution to the solution.

The motivation to derive MSWE is straightforward: The SWE are hyperbolic-type partial differential equations so that the consideration of the front condition (1.1) at downstream is mathematically nonrigorous. But without (1.1), the ambient resistance is absent from the formulation. We therefore rederive the governing equations by taking the ambient resistance into account. The resultant MSWE are parabolic-type differential equations in which the ambient resistance is accounted for by a nonlinear term. To solve the parabolic MSWE, boundary conditions are needed both upstream and downstream. To the outer equations, the upstream boundary condition is the source condition (1.4) and the downstream boundary condition is the matching condition at the interface between the outer and inner regions. To the inner equations, the upstream boundary condition is the matching condition and the downstream condition is the contact angle at the contact point ($h=0$), given as $\theta_c\approx 90°$. As a consequence, the MSWE lead to a composite solution for the entire current, which has the following features:

(1) The outer solutions turn out to be exactly the same as those obtained by solving the convectional SWE (1.2) and (1.3) together with the front condition (1.1).

(2) The inner solution, independent of the release condition at the current source, describes both the profile and the velocity of the current head. It also leads to a new front condition (3.26), a function of both density ratio γ and the contact angle θ_c, which is obtained as a part of the inner solution.

TABLE I. Summary of the solutions of MSWE: constant volume current ($\alpha=0$) and constant flux current ($\alpha=1$).

	$\alpha=1$	$\alpha=0$	
Cases	Self-similar phase (Without hydraulic jumps)	Initial slumping stage	Self-similar phase (Without dry-region)
Outer solutions	$u=\begin{cases} u_0, & 0\leqslant x\leqslant x_s \\ \frac{2}{3}\frac{x}{t}+C_1u_0, & x\geqslant x_s \end{cases}$	$u=\begin{cases} 0, & x\leqslant x_s \\ \frac{2}{3}\frac{x}{t}+C_2\sqrt{g_rh_0}, & x\geqslant x_s \end{cases}$	$u=\frac{2}{3}\frac{x}{t}$
	$h=\begin{cases} h_0, & 0\leqslant x\leqslant x_s \\ g_r^{-1}\left[C_1u_0-\frac{1}{3}\frac{x}{t}\right]^2, & x\geqslant x_s \end{cases}$	$h=\begin{cases} h_0, & 0\leqslant x\leqslant x_s \\ g_r^{-1}\left[C_2\sqrt{g_rh_0}-\frac{1}{3}\frac{x}{t}\right]^2, & x\geqslant x_s \end{cases}$	$h=\frac{1}{9g_r}\left(\frac{x}{t}\right)^2+Kt^{-(2/3)}$
Inner solutions	$\begin{cases} u=u_f \\ h=h_0H_{(0)}(X,t') \end{cases}$	where $H_{(0)}$ is given by Eq. (3.21) numerically. The inner solutions recover the front condition $u_f=\sqrt{(\frac{2}{\gamma\Lambda})g_rh_f}$, in which $\Lambda=\frac{\tan^2\theta_c}{1+\tan^2\theta_c}$, $g_r=(1-\gamma)g$, and $\gamma=\rho_a/\rho$.	
Composite solution by matching	$u=\begin{cases} u_0 & 0\leqslant x\leqslant x_s \\ \frac{2}{3}\frac{x}{t}+C_1u_0 & x_s\leqslant x\leqslant x_n \\ \frac{3\beta}{(2+\beta)}C_1u_0 & x_n\leqslant x\leqslant x_f \end{cases}$	$u=\begin{cases} 0 & x\leqslant x_s \\ \frac{2}{3}\frac{x}{t}+C_2\sqrt{g_rh_0} & x_s\leqslant x\leqslant x_n \\ \frac{2\beta}{(2+\beta)}\sqrt{g_rh_0} & x_n\leqslant x\leqslant x_f \end{cases}$	$u=\begin{cases} \frac{2}{3}\frac{x}{t}, & 0\leqslant x<x_m \\ 2\beta\sqrt{\frac{Kg_r}{4-\beta^2}}t^{-(1/3)} & x_m\leqslant x\leqslant x_f \end{cases}$
	$h=\begin{cases} h_0 & 0\leqslant x\leqslant x_s \\ g_r^{-1}\left[C_1u_0-\frac{1}{3}\frac{x}{t}\right]^2 & x_s\leqslant x\leqslant x_n \\ h_0H_{(0)} & x_n\leqslant x\leqslant x_f \end{cases}$	$h=\begin{cases} h_0 & x\leqslant x_s \\ g_r^{-1}\left[C_2\sqrt{g_rh_0}-\frac{1}{3}\frac{x}{t}\right]^2 & x_s\leqslant x\leqslant x_n \\ h_0H_{(0)} & x_n\leqslant x\leqslant x_f \end{cases}$	$h=\begin{cases} \frac{1}{9g_r}\left(\frac{x}{t}\right)^2+Kt^{-(2/3)}, & 0\leqslant x\leqslant x_m \\ h_0H_{(0)}, & x_m\leqslant x\leqslant x_f \end{cases}$
Constants	$C_1=\frac{\beta_0+2}{3\beta_0}$	$C_2=\frac{2}{3}$	$K=\frac{4-\beta^2}{(12\beta-2\beta^3)^{2/3}}V_0^{2/3}g_r^{-1/3}$
Some conjugate points	$x_s=\frac{\beta_0-1}{\beta_0}u_0t$	$x_s=-\sqrt{g_rh_0}t$	$x_m=x_n=3\beta\sqrt{\frac{Kg_r}{4-\beta^2}}t^{2/3}$
Values at the front	$x_n=3C_1\frac{\beta-1}{\beta+2}u_0t$	$x_n=\frac{2\beta-2}{2+\beta}\sqrt{g_rh_0t}$	
	$u_f=\frac{3\beta}{2+\beta}C_1u_0$	$u_f=\frac{2\beta}{\beta+2}\sqrt{g_eh_0}$	$u_f=2\beta\sqrt{\frac{Kg_r}{4-\beta^2}}t^{-(1/3)}$
	$h_\infty=\left(\frac{3C_1}{\beta+2}\right)^2\frac{u_0^2}{g_r}$	$h_\infty=\left(\frac{2}{\beta+2}\right)^2h_0$	$h_\infty=\left(\frac{4}{4-\beta^2}\right)Kt^{-(2/3)}$

(3) The combination of inner and outer solutions gives the composite solution in analytical form (see Table I) for the entire gravity current, including domains of the far field and the head, which was described by Benjamin [3, p. 227] as a "formidably complicated" task.

To consider the turbulent drag on the current, we introduce the semiempirical Chezy drag term into MSWE and find that this term serves well to account for the viscous correction of the present approach. For Boussinesq currents having $\gamma\approx 1$, the inviscid MSWE can simulate the current

motion fairly well. For non-Boussinesq currents having small γ, the turbulent flow becomes vigorous so that the viscous drag effect is significant. As a result, the MSWE shall include the Chezy drag term so that the turbulent drag on the current can be taken into account.

We note that the solution for $\alpha=0$ at the initial stage (the dam-break case of Sec. IV A) is a special case of the solution for $\alpha=1$ as $\beta_0=0$, a case such that the flow velocity at the current source vanishes. This fits exactly the dam-break case (Fig. 8), implying that the solution procedures of these two cases are correct.

We also note that the present MSWE are valid for the gravity current intruding beneath an infinite ambient fluid but may be invalid for the "lock exchange" currents in a channel of finite depth. To derive the MSWE for lock exchange currents, the pressure P_t can no longer be considered as a constant. Consequently, the derivation starting from (2.9) shall be very different from the present ones and may end up with equations which are so complicated that they may not be solved analytically.

Finally, please note that the present MSWE are valid for two-dimensional planar or axisymmetric gravity currents. For many gravity currents observed in experiments and in nature, nonetheless, the flow around the current head is three-dimensional and has a vigorous variation in the spanwise direction at the current front. Since the inner solution of the current head is the major contribution of the present MSWE approach, to solve the three-dimensional MSWE accordingly shall merit further study. The derivation of the three-dimensional MSWE is shown in Appendix C.

ACKNOWLEDGMENTS

We thank Professor K. Hutter of the Technical University of Damstadt for his kind help on English correction of the manuscript. Financial support from National Science Council of Taiwan under Grant No. NSC 92-2212-E-002-024 is gratefully acknowledged.

APPENDIX A: THE DERIVATION OF THE UNSTEADY FORCE TERM OF (2.9)

The unsteady force term of (2.9), or the term containing ϕ, cannot be determined exactly except to be simplified further by neglecting w_t. To simplify this term, a crucial differential identity is needed for the whole derivation. First, let us consider

$$\left.\frac{\partial \phi}{\partial t}\right|_{y=h} = \frac{\partial}{\partial t}(\phi|_{y=h(x,t)}) - \left.\frac{\partial \phi}{\partial y}\right|_{y=h}\frac{\partial h}{\partial t}, \tag{A1}$$

so that

$$\frac{\partial}{\partial x}\left[\left.\frac{\partial \phi}{\partial t}\right|_{y=h}\right] = \frac{\partial}{\partial x}\left[\frac{\partial}{\partial t}(\phi|_{y=h}) - \left.\frac{\partial \phi}{\partial y}\right|_{y=h}\frac{\partial h}{\partial t}\right] = \frac{\partial^2}{\partial x \partial t}(\phi|_{y=h}) - \frac{\partial}{\partial x}\left(\left.\frac{\partial h}{\partial t}\frac{\partial \phi}{\partial y}\right|_{y=h}\right). \tag{A2}$$

The first term on the right-hand side of (A2) can be further expanded as follows:

$$\frac{\partial^2(\phi|_{y=h})}{\partial x \partial t} = \frac{\partial}{\partial t}\frac{\partial(\phi|_{y=h})}{\partial x} = \frac{\partial}{\partial t}\left[\left.\frac{\partial \phi}{\partial x}\right|_{y=h} + \left.\frac{\partial \phi}{\partial y}\right|_{y=h}\frac{\partial h}{\partial x}\right] = \frac{\partial}{\partial t}\left[\vec{V}_i \cdot \left(\vec{e}_x + \frac{\partial h}{\partial x}\vec{e}_y\right)\right], \tag{A3}$$

in which the identity of velocity potential $\vec{V}=\nabla\phi$ has been used. By neglecting w_t in (A3), we obtain

$$\frac{\partial^2(\phi|_{y=h})}{\partial x \partial t} \approx \frac{\partial}{\partial t}\left[w_n \vec{e}_n \cdot \left(\vec{e}_x + \frac{\partial h}{\partial x}\vec{e}_y\right)\right] = 0, \tag{A4}$$

in which $\vec{e}_n=-h_{,x}\vec{e}_x+\vec{e}_y/\sqrt{h_{,x}^2+1}$ and (2.8) have been used. As for the second term on the right-hand side of (A2), we first consider

$$\left.\frac{\partial \phi}{\partial y}\right|_{y=h} = \nabla\phi|_{y=h}\cdot\vec{e}_y = \vec{V}_i\cdot\vec{e}_y \approx w_n\vec{e}_n\cdot\vec{e}_y = \frac{h_{,t}}{1+h_{,x}^2}. \tag{A5}$$

Accordingly,

$$\frac{\partial}{\partial x}\left(\left.\frac{\partial h}{\partial t}\frac{\partial \phi}{\partial y}\right|_{y=h}\right) = \frac{\partial}{\partial x}\left[\frac{h_{,t}^2}{1+h_{,x}^2}\right]. \tag{A6}$$

After substituting (A4) and (A6) into (A2), we eventually obtain

$$\frac{\partial}{\partial x}\left[\left.\frac{\partial \phi}{\partial t}\right|_{y=h(x,t)}\right] \approx -\frac{\partial}{\partial x}\left[\frac{h_{,t}^2}{1+h_{,x}^2}\right] = -\frac{\partial w_n^2}{\partial x}. \tag{A7}$$

Obviously, the variation of the potential function derived from the change of the interface turns out to be of the same form as that of the dynamic pressure.

APPENDIX B: DISCUSSION ABOUT THE ASCENDING AND DESCENDING SOLUTIONS

The matching procedure for the descending solutions of Sec. III A is applied to obtain the ascending solutions, and the results are summarized in Table II, in which both descending and ascending solutions at three positions x_s, x_n, and x_m are shown in the first three rows and those in the last two rows are shown for the discussion about the possibility in physical sense of the solutions.

We note that the variables in both the fourth and fifth rows must be larger than zero due to the fact that $x_m \geqslant x_n \geqslant x_s \geqslant 0$. For the descending solutions, $x_m \geqslant x_n \geqslant x_s$ can be satisfied when $\beta \geqslant \beta_0$, which satisfies automatically the condition $\beta \geqslant \beta_0 \geqslant 1$ concluded by Gratton and Vigo [13], so that the descending solutions are physically possible. For the ascending solutions, if $x_m \geqslant x_n$ holds, there shall be $\beta_0 \geqslant \beta > 2$ or $\beta_0 \leqslant \beta < 2$; if $x_n \geqslant x_s$ holds, there shall be $\beta_0 \geqslant 2 > \beta$ or $\beta_0 \leqslant 2 < \beta$. These two cases lead to conflicting results so that the ascending solutions are physically impossible.

APPENDIX C: DERIVATION OF THREE-DIMENSIONAL MSWE

The present approach deriving the two-dimensional MSWE can also be applied to derive the three-dimensional

TABLE II. Descending and ascending solutions of the gravity current at three points and two relations derived for the discussion about physical possibilities.

	Descending currents	Ascending currents
$x_s/u_0t=$	$\frac{\beta_0-1}{\beta_0}$	$\frac{\beta_0+1}{\beta_0}$
$x_n/u_0t=$	$\frac{(\beta_0+2)(\beta-1)}{\beta_0(2+\beta)}$	$\frac{(\beta_0-2)(\beta+1)}{\beta_0(\beta-2)}$
$x_m/u_0t=$	$\frac{(\beta_0+2)\beta}{\beta_0(\beta+2)}$	$\frac{(\beta_0-2)\beta}{\beta_0(\beta-2)}$
$(x_n-x_s)/u_0t=$	$\frac{3(\beta-\beta_0)}{\beta_0(\beta+2)}$	$\frac{3(\beta_0-\beta)}{\beta_0(\beta-2)}$
$(x_m-x_n)/u_0t=$	$\frac{\beta_0+2}{\beta_0(\beta+2)}$	$\frac{2-\beta_0}{\beta_0(\beta-2)}$
Physical sense	*Possible*	*Impossible*

counterpart in the Cartesian coordinate system. By neglecting mixing entrainment and surface tension at the interface and by assuming that the velocities in both the x and y directions are uniform, the kinematic condition is employed to simplify the mass conservation into

$$\frac{\partial h}{\partial t}+\frac{\partial(uh)}{\partial x}+\frac{\partial(vh)}{\partial y}=0, \tag{C1}$$

where $h=h(x,y,t)$ is the depth of the shallow-water layer. After neglecting the vertical acceleration, the momentum equation in z direction leads to a hydrostatic pressure distribution, given by

$$P(x,y,z,t)=P_i(x,y,t)+\rho g(h-z), \tag{C2}$$

where $P_i(x,y,t)$ denotes the interfacial pressure. After applying Bernoulli's equations along the instant streamline emitting from the interface, P_i can be expressed as

$$P_i=P_t-\rho_a gh-\frac{1}{2}\rho_a(\vec{V}_i)^2-\rho_a\left.\frac{\partial\phi}{\partial t}\right|_{z=h(x,y,t)}, \tag{C3}$$

where ρ_a and $\vec{V}_i$ are the density and the velocity of the ambient fluid, respectively, and $\phi=\phi(x,y,z,t)$ is the velocity potential. Note that the total pressure P_t is constant if the domain of the ambient fluid is infinite. Using (C2) and (C3) results in the momentum equations in the x and y directions, given respectively by

$$\frac{\partial u}{\partial t}+u\frac{\partial u}{\partial x}+v\frac{\partial u}{\partial y}+g_r\frac{\partial h}{\partial x}=\frac{\gamma}{2}\frac{\partial(\vec{V}_i)^2}{\partial x}+\gamma\frac{\partial}{\partial x}\left[\left.\frac{\partial\phi}{\partial t}\right|_{z=h(x,y,t)}\right], \tag{C4}$$

$$\frac{\partial v}{\partial t}+u\frac{\partial v}{\partial x}+v\frac{\partial v}{\partial y}+g_r\frac{\partial h}{\partial y}=\frac{\gamma}{2}\frac{\partial(\vec{V}_i)^2}{\partial y}+\gamma\frac{\partial}{\partial y}\left[\left.\frac{\partial\phi}{\partial t}\right|_{z=h(x,y,t)}\right]. \tag{C5}$$

We follow the approach of Sec. II to simplify the two terms on the right side of the above two equations. The derivation procedures of these two terms are similar with those shown in Sec. II and Appendix B. Consequently, we obtain the three-dimensional MSWE as follows:

$$\frac{\partial u}{\partial t}+u\frac{\partial u}{\partial x}+v\frac{\partial u}{\partial y}+g_r\frac{\partial h}{\partial x}=-\frac{\gamma}{2}\frac{\partial}{\partial x}\left[\frac{h_{,t}^2}{1+h_{,x}^2+h_{,y}^2}\right], \tag{C6}$$

$$\frac{\partial v}{\partial t}+u\frac{\partial v}{\partial x}+v\frac{\partial v}{\partial y}+g_r\frac{\partial h}{\partial y}=-\frac{\gamma}{2}\frac{\partial}{\partial y}\left[\frac{h_{,t}^2}{1+h_{,x}^2+h_{,y}^2}\right]. \tag{C7}$$

Equations (C1), (C6), and (C7) are three simultaneous partial differential equations for u, v, and h, governing the three-dimensional motion of inviscid gravity currents intruding into an unbounded ambient fluid. Equations (C1) and (C6) can be degenerated into the two-dimensional counterparts (2.2) and (2.11) if we drop all terms involving the derivative with respect to y.

We note that in the previous studies using analytical approaches mentioned in Sec. I, only two-dimensional gravity currents were considered due to the limitation of the front condition. There have been a few studies considering three-dimensional gravity currents, however, only for limiting cases with numerical solutions. For example, Hartel *et al.* [21] solved three-dimensional Navier-Stokes equations for Boussinesq currents ($\gamma\approx 1$) by direct numerical simulation scheme, and Zoppou and Roberts [22] investigated a three-dimensional dam-break problem ($\gamma\approx 0$) by solving shallow-

-water equations with a finite-difference approach. To the best of our knowledge, there has been no analytical approach ever applied to three-dimensional gravity currents for arbitrary density contrast.

The present three-dimensional MSWE may provide a good tool to study three-dimensional gravity currents analytically. The same approach, i.e., the asymptotic inner-outer expansion, can be applied when the current is separated into the far field and the near field. It is inferred that in the far field the three-dimensional effect can be negligible so that the two-dimensional results apply. In the near field, nevertheless, due to the vigorous variation in the spanwise direction in the current head, the inner equations shall be simplified further, as in Sec. III C, in order that the inner solutions can be matched with the outer counterparts. The spanwise variation of the current head can be possibly obtained only if the variation at the current front in terms of physical parameters such as the contact angle is properly fitted into the model.

[1] J. E. Simpson, *Gravity Currents in the Environment and in the Laboratory*, 1st ed. (Cambridge University Press, Cambridge England; 1st ed., 1987, Ellis-Horwood, Chichester, 1997).
[2] H. P. Groebelbauer, T. K. Fannelop, and R. E. Britter, J. Fluid Mech. **250**, 669 (1993).
[3] T. B. Benjamin, J. Fluid Mech. **31**, 209 (1968).
[4] J. B. Klemp, R. Rotunno, and W. C. Skamarock, J. Fluid Mech. **269**, 169 (1994).
[5] R. E. Grundy and J. W. Rottman, J. Fluid Mech. **156**, 39 (1985).
[6] T. K. Fannelop and G. D. Waldman, AIAA J. **10**, 506 (1971).
[7] D. P. Hoult, Annu. Rev. Fluid Mech. **4**, 341 (1972).
[8] R. E. Britter, Atmos. Environ. **13**, 1241 (1979).
[9] J. W. Rottman and J. E. Simpson, J. Fluid Mech. **135**, 95 (1983).
[10] R. E. Grundy and J. W. Rottman, J. Fluid Mech. **169**, 337 (1986).
[11] F. Chen, Appl. Mech. Rev. **53**(8), 207 (2000).
[12] A. C. Slim and H. E. Huppert, J. Fluid Mech. **506**, 331 (2004).
[13] J. Gratton and C. Vigo, J. Fluid Mech. **258**, 77 (1994).
[14] K. K. Droegemeier and R. B. Wilhelmson, J. Atmos. Sci. **44**, 1180 (1987).
[15] A. J. Hogg and D. Pritchard, J. Fluid Mech. **501**, 179 (2004).
[16] C. C. Mei, in Lecture Notes Chap. 2 (http://web.mit.edu/1.63/www/lecnote.html) (2001).
[17] T. von Karman, Bull. Am. Math. Soc. **46**, 615 (1940).
[18] J. E. Simpson and R. E. Britter, J. Fluid Mech. **94**, 477 (1979).
[19] P. K. Stansby, A. Chegini, and T. C. D. Barnes, J. Fluid Mech. **374**, 407 (1998).
[20] J. A. Fay, in *Oil on the Sea* (Plenum, New York, 1969), p. 46.
[21] C. Hartel, E. Meiburg, and F. Necker, J. Fluid Mech. **418**, 189 (2000).
[22] C. Zoppou and S. Roberts, Appl. Math. Model. **24**, 457 (2000).